

DIFFERENTIATE EVERYTHING WITH A REVERSIBLE EMBEDDED DOMAIN-SPECIFIC LANGUAGE

Anonymous authors

Paper under double-blind review

ABSTRACT

Reverse-mode automatic differentiation (AD) suffers from the issue of having too much space overhead to trace back intermediate computational states for back-propagation. The traditional method to trace back states is called checkpointing that stores intermediate states into a global stack and restore state through either stack pop or re-computing. The overhead of stack manipulations and re-computing makes the general purposed (not tensor-based) AD engines unable to meet many industrial needs. Instead of checkpointing, we propose to use reverse computing to trace back states by designing and implementing a reversible programming eDSL, where a program can be executed bi-directionally without implicit stack operations. The absence of implicit stack operations makes the program compatible with existing compiler features, including utilizing existing optimization passes and compiling the code as GPU kernels. We implement AD for sparse matrix operations and some machine learning applications to show that our framework has the state-of-the-art performance.

1 INTRODUCTION

Most of the popular automatic differentiation (AD) tools in the market, such as TensorFlow (Abadi et al., 2015), Pytorch (Paszke et al., 2017), and Flux (Innes et al., 2018) implements reverse mode AD at the tensor level to meet the need in machine learning. Later, People in the scientific computing domain also realized the power of these AD tools, they use these tools to solve scientific problems such as seismic inversion (Zhu et al., 2020), variational quantum circuits simulation (Bergholm et al., 2018; Luo et al., 2019) and variational tensor network simulation (Liao et al., 2019; Roberts et al., 2019). To meet the diverse need in these applications, one sometimes has to define backward rules manually, for example

1. To differentiate sparse matrix operations used in Hamiltonian engineering (Hao Xie & Wang), people defined backward rules for sparse matrix multiplication and dominant eigensolvers (Golub & Van Loan, 2012),
2. In tensor network algorithms to study the phase transition problem (Liao et al., 2019; Seeger et al., 2017; Wan & Zhang, 2019; Hubig, 2019), people defined backward rules for singular value decomposition (SVD) function and QR decomposition (Golub & Van Loan, 2012).

Instead of defining backward rules manually, one can also use a general purposed AD (GP-AD) framework like Tapenade (Hascoet & Pascual, 2013), OpenAD (Utke et al., 2008) and Zygote (Innes, 2018; Innes et al., 2019). Researchers have used these tools in practical applications such as bundle adjustment (Shen & Dai, 2018) and earth system simulation (Forget et al., 2015), where differentiating scalar operations is important. However, the power of these tools are often limited by their relatively poor performance. In many practical applications, a program might do billions of computations. In each computational step, the AD engine might cache some data for backpropagation. (Griewank & Walther, 2008) Frequent caching of data slows down the program significantly, while the memory usage will become a bottleneck as well. Caching implicitly also make these frameworks incompatible with kernel functions. To avoid such issues, we need a new GP-AD framework that does not cache automatically for users.

In this paper, we propose to implement the reverse mode AD on a reversible (domain-specific) programming language (Perumalla, 2013; Frank, 2017), where intermediate states can be traced

backward without accessing an implicit stack. Reversible programming allows people to utilize the reversibility to reverse a program. In machine learning, reversibility is proven to substantially decrease the memory usage in unitary recurrent neural networks (MacKay et al., 2018), normalizing flow (Dinh et al., 2014), hyper-parameter learning (Maclaurin et al., 2015) and residual neural networks (Gomez et al., 2017; Behrmann et al., 2018). Reversible programming will make these happen naturally. The power of reversible programming is not limited to handling these reversible applications, any program can be written in a reversible style. Converting an irreversible program to the reversible form would cost overheads in time and space. Reversible programming provides a flexible time-space trade-off scheme that different with checkpointing (Griewank, 1992; Griewank & Walther, 2008; Chen et al., 2016), *reverse computing* (Bennett, 1989; Levine & Sherman, 1990), to let user handle these overheads explicitly.

There have been many prototypes of reversible languages like Janus (Lutz, 1986), R (not the popular one) (Frank, 1997), Erlang (Lanese et al., 2018) and object-oriented ROOPL (Haulund, 2017). In the past, the primary motivation to study reversible programming is to support reversible computing devices (Frank & Knight Jr, 1999) such as adiabatic complementary metal-oxide-semiconductor (CMOS) (Koller & Athas, 1992), molecular mechanical computing system (Merkle et al., 2018) and superconducting system (Likharev, 1977; Semenov et al., 2003; Takeuchi et al., 2014; 2017), and these reversible computing devices are orders more energy-efficient. Landauer proves that only when a device does not erase information (i.e. reversible), its energy efficiency can go beyond the thermal dynamic limit. (Landauer, 1961; Reeb & Wolf, 2014) However, these reversible programming languages can not be used directly in real scientific computing, since most of them do not have basic elements like floating point numbers, arrays, and complex numbers. This motivates us to build a new embedded domain-specific language (eDSL) in Julia (Bezanson et al., 2012; 2017) as a new playground of GP-AD.

In this paper, we first introduce the language design of NiLang in Sec. 3. In Sec. 4, we explain the implementation of automatic differentiation in NiLang. In Sec. 5, we benchmark the performance of NiLang’s AD with other AD software and explain why it is fast.

2 REVERSE COMPUTING AS AN ALTERNATIVE OF CHECKPOINTING

Reverse computing and checkpointing share many similarities. Consider an irreversible program with pure forward computing time T and run-time memory S . Table 1 shows that both schemes suffer from a space overhead that linear to time when executing in time $O(T)$. In reversible computing, to reach a minimum space overhead of $O(S \log(T/S))$ (Bennett, 1989; Levine & Sherman, 1990; Perumalla, 2013), the program has a polynomial overhead in time. While in checkpointing, there can be no space overhead. Since one can just recompute from beginning to obtain any intermediate state with time complexity $O(T^2)$.

Method	most time efficient (Time/Space)	most space efficient (Time/Space)
Checkpointing	$O(T)/O(T + S)$	$O(T^2)/O(S)$
Reverse computing (worst case)	$O(T)/O(T + S)$	$O(T(\frac{T}{S})^{0.585})/O(S \log(\frac{T}{S}))$

Table 1: T and S are the time and space of the original irreversible program. We put a “worst case” after the “Reverse computing” because the reversibility of the original program is not utilized.

In practical using cases, we need to trade off space and time. The most successful checkpointing algorithm that is widely used in automatic differentiation is the treeverse algorithm in Fig. 1(a). Where the computational process is binomially partitioned into d sectors. At the beginning of each sector, a snapshot is stored in the main memory. The states in the last sector are retrieved by the above space-efficient $O(T^2)$ algorithm. After that, the last checkpoint can be freed. The remaining sectors are further partitioned into $d - l + 1$ sub-sectors, where l is the sector index counting from the tail. The earlier sectors have more quota of snapshots while the latter sectors have less so that the total number of snapshots remain the same. Recursively apply this treeverse algorithm t times

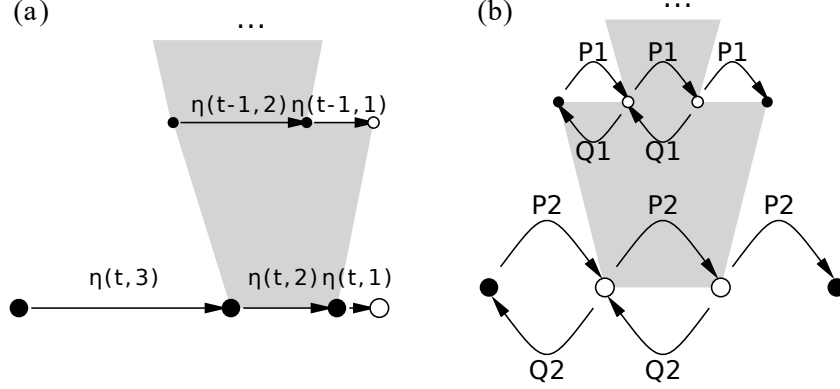


Figure 1: (a) Treeverse algorithm for optimal checkpointing. (Griewank, 1992) $\eta(\tau, \delta) \equiv \binom{\tau + \delta}{\delta} = \frac{(\tau + \delta)!}{\tau! \delta!}$ is the binomial function. (b) Bennett's time space trade-off scheme for reverse computing. (Bennett, 1973; Levine & Sherman, 1990) P and Q are computing and uncomputing respectively. The pseudo-code is defined in Listing. 1.

until the sector size is 1. The approximated overhead in time and space are

$$T_c = tT, S_c = dS. \quad (1)$$

Where $T = \eta(t, d)$. By carefully choosing either a t or d , the overhead in time and space can be both logarithmic.

On the other side, Bennett's trade-off of reverse computing also has a recursive structure as shown in Fig. 1 (b). But the program is evenly partitioned into k sectors. The program marches forward (P process) for k steps to obtain the final state s_{k+1} , then backward (Q process) from the $k - 1$ th step to erase the states in between $s_{1 < i \leq k}$. Each sector is further divided in to k sub-sectors and recursive run the above *compute-copy-uncompute* process. The time and space complexities are

$$T_r = T \left(\frac{T}{S} \right)^{\frac{\ln(2 - (1/k))}{\ln k}}, S_r = \frac{k - 1}{\ln k} S \log \frac{T}{S}. \quad (2)$$

Here, the overhead in time is polynomial, which is slightly worse than the treeverse algorithm. Treeverse like partition does not apply here because one can not complete the first sweep to create initial checkpoints without introducing any space overheads in reversible computing. The pseudo-code of Bennett's time-space trade-off algorithm is shown in Listing. 1. The first argument $\{s_1, \dots\}$ is the collection of states, k is the number of partitions, i and len are the starting point and length of the working sector. A function call changes variables inplace. " \sim " is the symbol of uncomputing, which means undoing a function call. Statement $s_{i+1} \leftarrow 0$ allocates a zero state and add it to the state collection. Its inverse $s_{i+1} \rightarrow 0$ discards a zero cleared state from the collection. The NiLang implementation is in Appendix A. Another interesting observation is reversible computing is not always more energy efficient irreversible computing. The time to uncompute a unit of memory is exponential to n as $Q_n = (2k - 1)^n$, and the computing energy also increases exponentially. On the other side, the amount of energy to erase a memory unit is constant. When $(2k - 1)^n > 1/\xi$, erasing the memory irreversibly is more energy-efficient, where ξ is the energy ratio between a reversible operation (an instruction or a gate) and its irreversible counterpart. For this reason, we think a reversible programming language is more suitable as an eDSL inside an irreversible host language rather than a stand-alone one. One can use the reversible operations at the microscopic level like registers and L1 cache level to save energy, and use the existing irreversible software stacks at the macroscopic level like the main memory level to discard information directly.

Listing 1: The Bennett’s time-space trade-off scheme.

```

bennett({s1,...}, k, i, len)
  if len == 1
    si+1 ← 0
    fi(si+1, si)
  else
    # P process that calls the forward program k steps
    bennett({s1,...}, k, i+len÷k*(j-1), len÷k) for j=1,2,...,k
    # Q process that calls the backward program k-1 steps
    ~bennett({s1,...}, k, i+len÷k*(j-1), len÷k) for j=k-1,k-2,...,1

```

The reverse computing does not show any advantage in worse-case complexity comparing with checkpointing. But the following traits make it perform better in many practical applications. *First*, it can make use of the reversibility to save memory. The above discussion assumes every operation is irreversible, however, the most program contains a lot of reversible instructions like the accumulation multiplication operations in many BLAS functions and sparse matrix functions. In Appendix B.2, we show how to implement a unitary matrix multiplication without introducing overheads in space and time. *Second*, reverse computing does not allocate automatically for users, user can optimize the memory access patterns for their own devices like GPU. *Third*, reverse computing can operate on effective codes, so that it fits better with modern languages. In Appendix B.1, we show how to manipulate inplace functions on arrays with NiLang. *Fourth*, reverse computing can utilize the existing compiler to optimize the code better because it does not automatically introduce global stack operations that harm the purity of functions. *Fifth*, reverse computing encourages the user to think reversibly. Reversible thinking can lead the user to a constant memory, constant time overhead implementation of chained multiplication algorithms as shown in Appendix B.3. Transpiling a regular code to a reversible code is not hard, but it is unlikely to provide the user with better performance than optimal checkpointing. Instead, thinking about how to write instructions and control flows reversibly does.

3 LANGUAGE DESIGN

NiLang is an embedded domain-specific language (eDSL) NiLang built on top of the host language Julia (Bezanson et al., 2012; 2017). Julia is a popular language for scientific programming and machine learning. We choose Julia mainly for speed. Julia is a language with high abstraction, however, its clever design of type inference and just in time compiling make it has a C like speed. Meanwhile, it has rich features for meta-programming. Its package for pattern matching [MLStyle](#) allows us to define an eDSL in less than 2000 lines. Comparing with a regular reversible programming language, NiLang features array operations, rich number systems including floating-point numbers, complex numbers, fixed-point numbers, and logarithmic numbers. It also implements the compute-copy-uncompute (Bennett, 1973) macro to increase code reusability. Besides the above reversible hardware compatible features, it also has some reversible hardware incompatible features to meet the practical needs. For example, it views the floating-point + and - operations as reversible. It also allows users to extend instruction sets and sometimes inserting external statements. These features are not compatible with future reversible hardware. NiLang’s source code is available online, we will put a link here after the anonymous open review session. By the time of writing, the version of NiLang is v0.7.3.

3.1 REVERSIBLE FUNCTIONS AND INSTRUCTIONS

Mathematically, any irreversible mapping $y = f(\text{args} \dots)$ can be trivially transformed to its reversible form $y += f(\text{args} \dots)$ or $y \vee= f(\text{args} \dots)$ (\vee is the bit-wise XOR), where y is a pre-empted variable. But in numeric computing with finite precision, this is not always true. The reversibility of arithmetic instruction is closely related to the number system. For integer and fixed point number system, $y += f(\text{args} \dots)$ and $y -= f(\text{args} \dots)$ are rigorously reversible. For logarithmic number system and tropical number system (Speyer & Sturmfels, 2009), $y *= f(\text{args} \dots)$ and $y /= f(\text{args} \dots)$ as reversible (not introducing the zero element). While for floating point numbers, none of the above operations are rigorously reversible. However, for convenience, we ignore the round-off errors in floating-point + and - operations and treat them on

equal footing with fixed-point numbers in the following discussion. In Appendix ??, we will show doing this is safe in most cases provided careful implementation. Other reversible operations includes SWAP, ROT, NEG et. al., and this instruction set is extensible. One can define a reversible multiplier in NiLang as in Listing. 2.

Listing 2: A reversible multiplier

```
julia> using NiLang

julia> @i function multiplier(y!::Real, a::Real, b::Real)
    y! += a * b
end

julia> multiplier(2, 3, 5)
(17, 3, 5)

julia> (~multiplier)(17, 3, 5)
(2, 3, 5)
```

Macro @i generates two functions that are reversible to each other, `multiplier` and `~multiplier`, each defines a mapping $\mathbb{R}^3 \rightarrow \mathbb{R}^3$. The ! after a symbol is a part of the name, as a conversion to indicate the mutated variables.

3.2 REVERSIBLE MEMORY MANAGEMENT

A distinct feature of reversible memory management is that the content of a variable must be known when it is deallocated. We denote the allocation of a pre-empted memory as $x \leftarrow \emptyset$, and its inverse, deallocating a **zero emptied** variable, as $x \rightarrow \emptyset$. An unknown variable can not be deallocate, but can be pushed to a stack pop out later in the uncomputing stage. If a variable is allocated and deallocated in the local scope, we call it an ancilla. Listing. 3 defines the complex valued accumulative log function.

Listing 3: Reversible complex valued log function $y += \log(|x|) + i\text{Arg}(x)$.

```
@i @inline function (:+=)(log)(y!::Complex{T}
    }, x::Complex{T}) where T
    n ← zero(T)
    n += abs(x)

    y!.re += log(n)
    y!.im += angle(x)

    n -= abs(x)
    n → zero(T)
end
```

Listing 4: Compute-copy-uncompute version of Listing. 3

```
@i @inline function (:+=)(log)(y!::Complex{T}
    }, x::Complex{T}) where T
    @routine begin
        n ← zero(T)
        n += abs(x)
    end
    y!.re += log(n)
    y!.im += angle(x)
    ~@routine
end
```

Here, the macro @inline tells the compiler that this function can be inlined. One can input “←” and “→” by typing “\leftarrow[TAB KEY]” and “\rightarrow[TAB KEY]” respectively in a Julia editor or REPL. NiLang does not have immutable structs, so that the real part `y!.re` and imaginary `y!.im` of a complex number can be changed directly. It is easy to verify that the bottom two lines in the function body are the inverse of the top two lines. i.e., the bottom two lines *uncomputes* the top two lines. The motivation of uncomputing is to zero clear the contents in ancilla `n` so that it can be deallocated correctly. *Compute-copy-uncompute* is a useful design pattern in reversible programming so that we created a pair of macros @routine and ~@routine for it. One can rewrite the above function as in Listing. 4.

3.3 REVERSIBLE CONTROL FLOWS

One can define reversible if, for and while statements in a reversible program. Fig. 2 (a) shows the flow chart of executing the reversible if statement. There are two condition expressions in

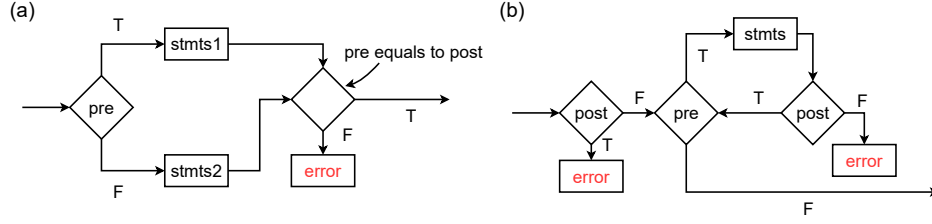


Figure 2: The flow chart for reversible (a) if statement and (b) while statement. “pre” and “post” represents precondition and postcondition respectively. The assertion errors are thrown to the host language instead of handling them in NiLang.

this chart, a precondition and a postcondition. The precondition decides which branch to enter in the forward execution, while the postcondition decides which branch to enter in the backward execution. The pseudo-code for the forward and backward passes are shown in Listing. 5 and Listing. 6.

Listing 5: Translating a reversible if statement (forward)

```
branchkeeper = precondition
if precondition
  branch A
else
  branch B
end
assert branchkeeper == postcondition
```

Listing 6: Translating a reversible if statement (backward)

```
branchkeeper = postcondition
if postcondition
  ~(branch A)
else
  ~(branch B)
end
assert branchkeeper == precondition
```

Fig. 2 (b) shows the flow chart of the reversible while statement. It also has two condition expressions. Before executing the condition expressions, the program presumes the postcondition is false. After each iteration, the program asserts the postcondition to be true. To reverse this statement, one can exchange the precondition and postcondition, and reverse the body statements. The pseudo-code for the forward and backward passes are shown in Listing. 7 and Listing. 8.

Listing 7: Translating a reversible while statement (forward)

```
assert postcondition == false
while precondition
  loop body
  assert postcondition == true
end
```

Listing 8: Translating a reversible while statement (backward)

```
assert precondition == false
while postcondition
  ~(loop body)
  assert precondition == true
end
```

The reversible for statement is similar to the irreversible one except that after execution, the program will assert the iterator to be unchanged. To reverse this statement, one can exchange start and stop and inverse the sign of step. Listing. 9 computes the Fibonacci number recursively and reversibly.

Listing 9: Computing Fibonacci number recursively and reversibly.

```

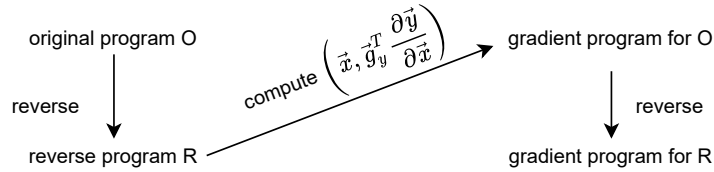
@i function rrfib(out!, n)
  @invcheckoff if (n >= 1, ~)
    counter ← 0
    counter += n
    while (counter > 1, counter!=n)
      rrfib(out!, counter-1)
      counter -= 2
    end
    counter -= n % 2
    counter → 0
  end
  out! += 1
end

```

Here, `out!` is an integer initialized to 0 for storing outputs. The precondition and postcondition are wrapped into a tuple. In the `if` statement, the postcondition is the same as the precondition, hence we omit the postcondition by inserting a `"~"` in the second field for “copying the precondition in this field as the postcondition”. In the `while` statement, the postcondition is true only for the initial loop. Once code is proven correct, one can turn off the reversibility check by adding `@invcheckoff` before a statement. This will remove the reversibility check and make the code faster and compatible with GPU kernels (kernel functions can not handle exceptions).

4 REVERSIBLE AUTOMATIC DIFFERENTIATION

4.1 BACK PROPAGATION



We decompose the problem of reverse mode AD into two sub-problems, **reversing the code** and **computing** $\frac{\partial[\text{single input}]}{\partial[\text{multiple outputs}]}$. Reversing the code is trivial in reversible programming, while the second sub-problem is similar to forward mode automatic differentiation that computes $\frac{\partial[\text{multiple outputs}]}{\partial[\text{single input}]}$. Inspired by the Julia package ForwardDiff (Revels et al., 2016), we use operator overloading rather than the source to source transformation for better extensibility. We wrap each output variable with a composite type `GVar` that containing an extra gradient field, and feed it into the reversed generic program. Instructions are multiple dispatched to corresponding gradient instructions that update the gradient field of `GVar` at the same time. By reversing this gradient program, we can obtain the gradient program for the reversed program `R` too. One can define the adjoint (“adjoint” here means a reversed program updating gradients) of a primitive instruction as a reversible function on **either** the function itself or its reverse since the adjoint of a function’s reverse is equivalent to the reverse of the function’s adjoint.

$$f : (\vec{x}, \vec{g}_x) \rightarrow (\vec{y}, \vec{g}_y^T \frac{\partial \vec{y}}{\partial \vec{x}}) \quad (3)$$

$$f^{-1} : (\vec{y}, \vec{g}_y) \rightarrow (\vec{x}, \vec{g}_x^T \frac{\partial \vec{y}}{\partial \vec{x}}) \quad (4)$$

It can be easily verified by applying the above two mappings consecutively, which turns out to be an identity mapping considering $\frac{\partial \vec{y}}{\partial \vec{x}} \frac{\partial \vec{x}}{\partial \vec{y}} = \mathbb{1}$.

The implementation details are described in Appendix C. In most languages, operator overloading brings significant overheads of function calls and object allocation and deallocation. But in a

language with type inference and just in time compiling like Julia, the boundary between two approaches are vague. The compiler inlines small functions, packs an array of constant sized immutable objects into a continuous memory, and truncates unnecessary branches automatically.

4.2 HESSIANS

Combining forward mode AD and reverse mode AD is a simple yet efficient way to obtain Hessians. By wrapping the elementary type with `Dual` defined in package `ForwardDiff` and throwing it into the gradient program defined in `NiLang`, one obtains one row/column of the Hessian matrix. We will use this approach to compute Hessians in the graph embedding benchmark in Sec. D.2.

4.3 CUDA KERNELS

CUDA programming is playing a significant role in high-performance computing. In Julia, one can write GPU compatible functions in native Julia language with `KernelAbstractions`. (Besard et al., 2017) Since `NiLang` does not push variables into stack automatically for users, it is safe to write differentiable GPU kernels with `NiLang`. We will differentiate CUDA kernels with no more than extra 10 lines in the bundle adjustment benchmark in Sec. 5.

5 BENCHMARKS

We benchmark our framework with the state-of-the-art GP-AD frameworks, including source code transformation based `Tapenade` and `Zygote` and operator overloading based `ForwardDiff` and `ReverseDiff`. Since most tensor based AD software like famous `TensorFlow` and `PyTorch` are not designed for the using cases used in our benchmarks, we do not include those package to avoid an unfair comparison. In the following benchmarks, the CPU device is Intel(R) Xeon(R) Gold 6230 CPU @ 2.10GHz, and the GPU device is NVIDIA Titan V. For `NiLang` benchmarks, we have turned the reversibility check off to achieve a better performance.

We reproduced the benchmarks for Gaussian mixture model (GMM) and bundle adjustment in [Srajer et al. \(2018\)](#) by re-writing the programs in a reversible style. We show the results in Fig. 3. The `Tapenade` data is obtained by executing the docker file provided by the original benchmark, which provides a baseline for comparison.

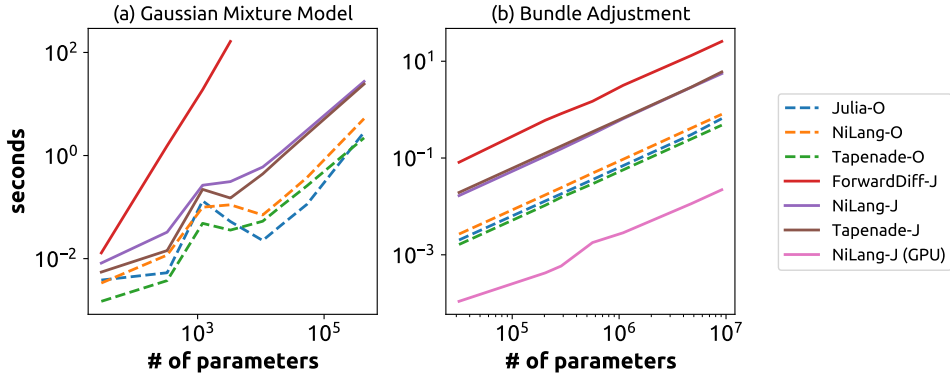


Figure 3: Absolute runtimes in seconds for computing the objective (-O) and Jacobians (-J). (a) GMM with 10k data points, the loss function has a single output, hence computing Jacobian is the same as computing gradient. ForwardDiff data is missing due to not finishing in limited time. The `NiLang` GPU data is missing because we do not write kernel here. (b) Bundle adjustment.

`NiLang`'s objective function is $\sim 2\times$ slower than normal code due to the uncomputing overhead. In this case, `NiLang` does not show advantage to `Tapenade` in obtaining gradients, the ratio between computing the gradients and the objective function are close. This is because the bottleneck of this model is the matrix vector multiplication, traditional AD can already handle this function well. The extra memory used to reverse the program is negligible comparing to the original program as shown

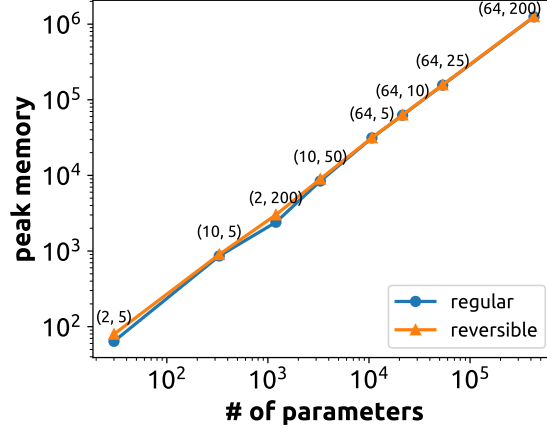


Figure 4: Peak memory of running the original and the reversible GMM program. The labels are (d, k) pairs.

in Fig. 4. The backward pass is not shown here, it is just two times the reversible program in order to store gradients. The data is obtained by counting the main memory allocations in the program manually. The analytical expression of memory usage in unit of floating point number is

$$S = (2 + d^2)k + 2d + P, \quad (5)$$

$$S_r = (3 + d^2 + d)k + 2\log_2 k + P, \quad (6)$$

where d and k are the size and number of covariance matrices. $P = \frac{d(d+1)}{2}k + k + dk$ is the size of parameter space. The memory of the dataset ($d \times N$) is not included because it will scale as N . Due to the hardness of estimating peak memory usage, the Tapenade data is missing here. The ForwardDiff memory usage is approximately the original size times the batch size, where the batch size is 12 by default.

In the bundle adjustment benchmark, NiLang performs the best on CPU. We also compiled our adjoint program to GPU with no more than 10 lines of code with KernelAbstractions, which provides another $\sim 200\times$ speed up. Parallelizing the adjoint code requires the forward code not reading the same variable simultaneously in different threads, and this requirement is satisfied here. The peak memory of the original program and the reversible program are both equal to the size of parameter space because all “allocation”’s happen on registers in this application.

One can find more benchmarks in Appendix D, including differentiating sparse matrix dot product and obtaining Hessians in the graph embedding application.

6 DISCUSSION

In this work, we demonstrate a new approach to back propagates a program called reversible programming AD by designing a reversible eDSL NiLang. NiLang is a powerful tool to differentiate code from the source code level so that can be directly useful to machine learning researches. It can generate efficient backward rules, which is exemplified in Appendix E. It can also be used to differentiate reversible neural networks like normalizing flows (Kobyzev et al., 2019) to save memory, e.g. back-propagating NICE network (Dinh et al., 2014) with only constant space overheads. Except for the above immediate benefits to the machine learning ecosystem, we also want to emphasize the broader impact of AD on reverse computing. AD on reverse computing is related to two of the central issues limiting many machine learning applications. One is how to overcome the memory wall that has been extensively discussed in the main text, and another is how to reduce energy consumption. AD on reverse computing provides a software stack that connecting machine learning with further technologies to save energy.

ACKNOWLEDGMENTS

The authors are grateful to the people who help improve this work and fundings that sponsored the research. To meet the anonymous criteria, we will add the acknowledgments after the open review session.

REFERENCES

- Martín Abadi, Ashish Agarwal, Paul Barham, Eugene Brevdo, Zhifeng Chen, Craig Citro, Greg S. Corrado, Andy Davis, Jeffrey Dean, Matthieu Devin, Sanjay Ghemawat, Ian Goodfellow, Andrew Harp, Geoffrey Irving, Michael Isard, Yangqing Jia, Rafal Jozefowicz, Lukasz Kaiser, Manjunath Kudlur, Josh Levenberg, Dandelion Mané, Rajat Monga, Sherry Moore, Derek Murray, Chris Olah, Mike Schuster, Jonathon Shlens, Benoit Steiner, Ilya Sutskever, Kunal Talwar, Paul Tucker, Vincent Vanhoucke, Vijay Vasudevan, Fernanda Viégas, Oriol Vinyals, Pete Warden, Martin Wattenberg, Martin Wicke, Yuan Yu, and Xiaoqiang Zheng. TensorFlow: Large-scale machine learning on heterogeneous systems, 2015. URL <https://www.tensorflow.org/>. Software available from tensorflow.org.
- Jens Behrmann, David Duvenaud, and Jörn-Henrik Jacobsen. Invertible residual networks. *CoRR*, abs/1811.00995, 2018. URL <http://arxiv.org/abs/1811.00995>.
- Charles H. Bennett. Logical reversibility of computation. 1973. URL <https://ieeexplore.ieee.org/abstract/document/5391327>.
- Charles H. Bennett. Time/space trade-offs for reversible computation. *SIAM Journal on Computing*, 18(4):766–776, 1989. doi: 10.1137/0218053. URL <https://doi.org/10.1137/0218053>.
- Ville Bergholm, Josh Izaac, Maria Schuld, Christian Gogolin, M. Sohaib Alam, Shah Nawaz Ahmed, Juan Miguel Arrazola, Carsten Blank, Alain Delgado, Soran Jahangiri, Keri McKiernan, Johannes Jakob Meyer, Zeyue Niu, Antal Száva, and Nathan Killoran. PennyLane: Automatic differentiation of hybrid quantum-classical computations, 2018. URL <https://arxiv.org/abs/1811.04968>.
- Tim Besard, Christophe Foket, and Bjorn De Sutter. Effective extensible programming: Unleashing julia on gpus. *CoRR*, abs/1712.03112, 2017. URL <http://arxiv.org/abs/1712.03112>.
- Jeff Bezanson, Stefan Karpinski, Viral B. Shah, and Alan Edelman. Julia: A fast dynamic language for technical computing, 2012. URL <https://arxiv.org/abs/1209.5145>.
- Jeff Bezanson, Alan Edelman, Stefan Karpinski, and Viral B. Shah. Julia: A fresh approach to numerical computing. *SIAM Review*, 59(1):65–98, Jan 2017. ISSN 1095-7200. doi: 10.1137/141000671. URL <http://dx.doi.org/10.1137/141000671>.
- Tianqi Chen, Bing Xu, Chiyuan Zhang, and Carlos Guestrin. Training deep nets with sublinear memory cost. *CoRR*, abs/1604.06174, 2016. URL <http://arxiv.org/abs/1604.06174>.
- Laurent Dinh, David Krueger, and Yoshua Bengio. Nice: Non-linear independent components estimation, 2014. URL <https://arxiv.org/abs/1410.8516>.
- GAEL Forget, J-M Campin, Patrick Heimbach, Christopher N Hill, Rui M Ponte, and Carl Wunsch. Ecco version 4: An integrated framework for non-linear inverse modeling and global ocean state estimation. 2015. URL <https://dspace.mit.edu/handle/1721.1/99660>.
- Michael P Frank. The r programming language and compiler. Technical report, MIT Reversible Computing Project Memo, 1997.
- Michael P. Frank. Throwing computing into reverse. *IEEE Spectrum*, 54(9):32–37, Sep 2017. ISSN 0018-9235. doi: 10.1109/mspec.2017.8012237. URL <http://dx.doi.org/10.1109/MSPEC.2017.8012237>.
- Michael Patrick Frank and Thomas F Knight Jr. *Reversibility for efficient computing*. PhD thesis, 1999. URL <http://citeseerx.ist.psu.edu/viewdoc/download?doi=10.1.1.428.4962&rep=rep1&type=pdf>.

Gene H Golub and Charles F Van Loan. *Matrix computations*, volume 3. JHU press, 2012.

Aidan N Gomez, Mengye Ren, Raquel Urtasun, and Roger B Grosse. The reversible residual network: Backpropagation without storing activations. In I. Guyon, U. V. Luxburg, S. Bengio, H. Wallach, R. Fergus, S. Vishwanathan, and R. Garnett (eds.), *Advances in Neural Information Processing Systems 30*, pp. 2214–2224. Curran Associates, Inc., 2017. URL <http://papers.nips.cc/paper/6816-the-reversible-residual-network-backpropagation-without-storing-activations.pdf>.

Andreas Griewank. Achieving logarithmic growth of temporal and spatial complexity in reverse automatic differentiation. *Optimization Methods and software*, 1(1):35–54, 1992. URL <https://www.tandfonline.com/doi/abs/10.1080/10556789208805505>.

Andreas Griewank and Andrea Walther. *Evaluating derivatives: principles and techniques of algorithmic differentiation*. SIAM, 2008.

Jin-Guo Liu Hao Xie and Lei Wang. Automatic differentiation of dominant eigensolver and its applications in quantum physics. URL <https://arxiv.org/abs/2001.04121>.

Laurent Hascoet and Valérie Pascual. The tapenade automatic differentiation tool: Principles, model, and specification. *ACM Transactions on Mathematical Software (TOMS)*, 39(3):20, 2013. URL <https://dl.acm.org/citation.cfm?id=2450158>.

Tue Haulund. Design and implementation of a reversible object-oriented programming language, 2017. URL <https://arxiv.org/abs/1707.07845>.

Claudius Hubig. Use and implementation of autodifferentiation in tensor network methods with complex scalars, 2019. URL <https://arxiv.org/abs/1907.13422>.

Michael Innes. Don’t unroll adjoint: Differentiating ssa-form programs, 2018. URL <https://arxiv.org/abs/1810.07951>.

Michael Innes, Elliot Saba, Keno Fischer, Dhairya Gandhi, Marco Concetto Rudilosso, Neethu Mariya Joy, Tejan Karmali, Avik Pal, and Viral Shah. Fashionable modelling with flux, 2018. URL <https://arxiv.org/abs/1811.01457>.

Mike Innes, Alan Edelman, Keno Fischer, Christopher Rackauckas, Elliot Saba, Viral B. Shah, and Will Tebbutt. A differentiable programming system to bridge machine learning and scientific computing. *CoRR*, abs/1907.07587, 2019. URL <http://arxiv.org/abs/1907.07587>.

Li Jing, Yichen Shen, Tena Dubcek, John Peurifoy, Scott Skirlo, Yann LeCun, Max Tegmark, and Marin Soljacić. Tunable efficient unitary neural networks (eunn) and their application to rnns, 2016. URL <https://arxiv.org/abs/1612.05231>.

Diederik P Kingma and Jimmy Ba. Adam: A method for stochastic optimization. URL <https://arxiv.org/abs/1412.6980>.

Ivan Kobyzev, Simon Prince, and Marcus A. Brubaker. Normalizing flows: An introduction and review of current methods, 2019.

J. G. Koller and W. C. Athas. Adiabatic switching, low energy computing, and the physics of storing and erasing information. In *Workshop on Physics and Computation*, pp. 267–270, Oct 1992. doi: 10.1109/PHYCMP.1992.615554. URL <https://ieeexplore.ieee.org/document/615554>.

Rolf Landauer. Irreversibility and heat generation in the computing process. *IBM journal of research and development*, 5(3):183–191, 1961. URL <https://ieeexplore.ieee.org/document/5392446>.

Ivan Lanese, Naoki Nishida, Adrián Palacios, and Germán Vidal. A theory of reversibility for erlang. *Journal of Logical and Algebraic Methods in Programming*, 100:71–97, Nov 2018. ISSN 2352-2208. doi: 10.1016/j.jlamp.2018.06.004. URL <http://dx.doi.org/10.1016/j.jlamp.2018.06.004>.

- Robert Y Levine and Alan T Sherman. A note on bennett’s time-space tradeoff for reversible computation. *SIAM Journal on Computing*, 19(4):673–677, 1990. URL <https://epubs.siam.org/doi/abs/10.1137/0219046>.
- Hai-Jun Liao, Jin-Guo Liu, Lei Wang, and Tao Xiang. Differentiable programming tensor networks. *Physical Review X*, 9(3), Sep 2019. ISSN 2160-3308. doi: 10.1103/physrevx.9.031041. URL <http://dx.doi.org/10.1103/PhysRevX.9.031041>.
- K. Likharev. Dynamics of some single flux quantum devices: I. parametric quantron. *IEEE Transactions on Magnetics*, 13(1):242–244, January 1977. ISSN 1941-0069. doi: 10.1109/TMAG.1977.1059351. URL <https://ieeexplore.ieee.org/document/1059351>.
- Xiu-Zhe Luo, Jin-Guo Liu, Pan Zhang, and Lei Wang. Yao.jl: Extensible, efficient framework for quantum algorithm design, 2019. URL <https://arxiv.org/abs/1912.10877>.
- Christopher Lutz. Janus: a time-reversible language. *Letter to R. Landauer.*, 1986.
- Matthew MacKay, Paul Vicol, Jimmy Ba, and Roger B Grosse. Reversible recurrent neural networks. In S. Bengio, H. Wallach, H. Larochelle, K. Grauman, N. Cesa-Bianchi, and R. Garnett (eds.), *Advances in Neural Information Processing Systems 31*, pp. 9029–9040. Curran Associates, Inc., 2018. URL <http://papers.nips.cc/paper/8117-reversible-recurrent-neural-networks.pdf>.
- Dougal Maclaurin, David Duvenaud, and Ryan Adams. Gradient-based hyperparameter optimization through reversible learning. In Francis Bach and David Blei (eds.), *Proceedings of the 32nd International Conference on Machine Learning*, volume 37 of *Proceedings of Machine Learning Research*, pp. 2113–2122, Lille, France, 07–09 Jul 2015. PMLR. URL <http://proceedings.mlr.press/v37/maclaurin15.html>.
- Ralph C. Merkle, Robert A. Freitas, Tad Hogg, Thomas E. Moore, Matthew S. Moses, and James Ryley. Mechanical computing systems using only links and rotary joints. *Journal of Mechanisms and Robotics*, 10(6), Sep 2018. ISSN 1942-4310. doi: 10.1115/1.4041209. URL <http://dx.doi.org/10.1115/1.4041209>.
- Adam Paszke, Sam Gross, Soumith Chintala, Gregory Chanan, Edward Yang, Zachary DeVito, Zeming Lin, Alban Desmaison, Luca Antiga, and Adam Lerer. Automatic differentiation in PyTorch. In *NIPS Autodiff Workshop*, 2017. URL <https://openreview.net/forum?id=BJJsrnmcZ>.
- Kalyan S Perumalla. *Introduction to reversible computing*. Chapman and Hall/CRC, 2013.
- David Reeb and Michael M Wolf. An improved landauer principle with finite-size corrections. *New Journal of Physics*, 16(10):103011, 2014. URL <https://iopscience.iop.org/article/10.1088/1367-2630/16/10/103011/meta>.
- Jarrett Revels, Miles Lubin, and Theodore Papamarkou. Forward-mode automatic differentiation in julia, 2016. URL <https://arxiv.org/abs/1607.07892>.
- Chase Roberts, Ashley Milsted, Martin Ganahl, Adam Zalcman, Bruce Fontaine, Yijian Zou, Jack Hidary, Guifre Vidal, and Stefan Leichenauer. Tensornetwork: A library for physics and machine learning, 2019. URL <https://arxiv.org/abs/1905.01330>.
- Matthias Seeger, Asmus Hetzel, Zhenwen Dai, Eric Meissner, and Neil D. Lawrence. Auto-differentiating linear algebra, 2017. URL <https://arxiv.org/abs/1710.08717>.
- V. K. Semenov, G. V. Danilov, and D. V. Averin. Negative-inductance squid as the basic element of reversible josephson-junction circuits. *IEEE Transactions on Applied Superconductivity*, 13(2):938–943, June 2003. ISSN 2378-7074. doi: 10.1109/TASC.2003.814155. URL <https://ieeexplore.ieee.org/document/1211760>.
- Yan Shen and Yuxing Dai. Fast automatic differentiation for large scale bundle adjustment. *IEEE Access*, 6:11146–11153, 2018. URL <https://ieeexplore.ieee.org/abstract/document/8307241/>.

David Speyer and Bernd Sturmfels. Tropical mathematics. *Mathematics Magazine*, 82(3):163–173, 2009. URL <https://www.tandfonline.com/doi/pdf/10.1080/0025570X.2009.11953615>.

Filip Srajer, Zuzana Kukelova, and Andrew Fitzgibbon. A benchmark of selected algorithmic differentiation tools on some problems in computer vision and machine learning. *Optimization Methods and Software*, 33(4-6):889–906, 2018. URL <https://openreview.net/forum?id=SMCWZLzTGDN>.

Jun Takahashi and Anders W. Sandvik. Valence-bond solids, vestigial order, and emergent $so(5)$ symmetry in a two-dimensional quantum magnet, 2020. URL <https://arxiv.org/abs/2001.10045>.

N Takeuchi, Y Yamanashi, and N Yoshikawa. Reversible logic gate using adiabatic superconducting devices. *Scientific reports*, 4:6354, 2014. URL <https://www.nature.com/articles/srep06354>.

Naoki Takeuchi, Yuki Yamanashi, and Nobuyuki Yoshikawa. Reversibility and energy dissipation in adiabatic superconductor logic. *Scientific reports*, 7(1):1–12, 2017. URL <https://www.nature.com/articles/s41598-017-00089-9>.

Clay S Turner. A fast binary logarithm algorithm [dsp tips & tricks]. *IEEE Signal Processing Magazine*, 27(5):124–140, 2010. URL <http://www.claysturner.com/dsp/binarylogarithm.pdf>.

Jean Utke, Uwe Naumann, Mike Fagan, Nathan Tallent, Michelle Strout, Patrick Heimbach, Chris Hill, and Carl Wunsch. Openad/f: A modular open-source tool for automatic differentiation of fortran codes. *ACM Trans. Math. Softw.*, 34(4), July 2008. ISSN 0098-3500. doi: 10.1145/1377596.1377598. URL <https://doi.org/10.1145/1377596.1377598>.

Zhou-Quan Wan and Shi-Xin Zhang. Automatic differentiation for complex valued svd, 2019. URL <https://arxiv.org/abs/1909.02659>.

Weiqiang Zhu, Kailai Xu, Eric Darve, and Gregory C. Beroza. A general approach to seismic inversion with automatic differentiation, 2020. URL <https://arxiv.org/abs/2003.06027>.

A NiLang IMPLEMENTATION OF BENNETT’S TIME-SPACE TRADE-OFF ALGORITHM

Listing 10: NiLang implementation of the Bennett’s time-space trade-off scheme.

```

using NiLang, Test

PROG_COUNTER = Ref{0} # (2k-1)^n
PEAK_MEM = Ref{0} # n*(k-1)+2

@i function bennett(f::AbstractVector, state::Dict{Int,T}, k::Int, base, len) where T
    if (len == 1, ~)
        state[base+1] ← zero(T)
        f[base](state[base+1], state[base])
        @safe PROG_COUNTER[] += 1
        @safe (length(state) > PEAK_MEM[] && (PEAK_MEM[] = length(state)))
    else
        n ← 0
        n += len÷k
        # the P process
        for j=1:k
            bennett(f, state, k, base+n*(j-1), n)
        end
        # the Q process
        for j=k-1:-1:1
            ~bennett(f, state, k, base+n*(j-1), n)
        end
        n -= len÷k
        n → 0
    end
end

k = 4
n = 4
N = k ^ n
state = Dict{1=>1.0}
f(x) = x * 2.0
instructions = fill(PlusEq(f), N)

# run the program
@instr bennett(instructions, state, k, 1, N)

@test state[N+1] ≈ 2.0^N && length(state) == 2
@test PEAK_MEM[] == n*(k-1) + 2
@test PROG_COUNTER[] == (2*k-1)^n

```

The input f is a vector of functions and $state$ is a dictionary. We also added some irreversible external statements (those marked with @safe) to help analyse to program.

B CASES WHERE REVERSE COMPUTING SHOWS ADVANTAGE

B.1 HANDLING EFFECTIVE CODES

Reverse computing can handling effective codes with mutable structures and arrays. For example, the affine transformation can be implemented without any overhead.

Listing 11: Inplace affine transformation.

```

@i function i_affine!(y!::AbstractVector{T}, W::AbstractMatrix{T}, b::AbstractVector{T}, x:
    :AbstractVector{T}) where T
    @safe @assert size(W) == (length(y!), length(x)) && length(b) == length(y!)
    @invcheckoff for j=1:size(W, 2)
        for i=1:size(W, 1)
            @inbounds y![i] += W[i,j]*x[j]
        end
    end
    @invcheckoff for i=1:size(W, 1)
        @inbounds y![i] += b[i]
    end
end

```

Here, the expression following the @safe macro is an external irreversible statement.

B.2 UTILIZING REVERSIBILITY

Reverse computing can utilize reversibility to trace back states without extra memory cost. For example, we can define the unitary matrix multiplication that can be used in a type of memory-efficient recurrent neural network. (Jing et al., 2016)

Listing 12: Two level decomposition of a unitary matrix.

```

@i function i_umm!(x!::AbstractArray, θ)
    M ← size(x!, 1)
    N ← size(x!, 2)
    k ← 0
    @safe @assert length(θ) == M*(M-1)/2
    for l = 1:N
        for j=1:M
            for i=M-1:-1:j
                INC(k)
                ROT(x![i,l], x![i+1,l], θ[k])
            end
        end
    end
    k → length(θ)
end

```

B.3 ENCOURAGES REVERSIBLE THINKING

Last but not least, reversible programming encourages users to code in a memory friendly style. Since allocations in reversible programming are explicit, programmers have the flexibility to control how to allocate memory and which number system to use. For example, to compute the power of a positive fixed-point number and an integer, one can easily write irreversible code as in Listing. 13

Listing 13: A regular power function.

```

function mypower(x::T, n::Int) where T
    y = one(T)
    for i=1:n
        y *= x
    end
    return y
end

```

Listing 14: A reversible power function.

```

@i function mypower(out, x::T, n::Int) where T
    if (x != 0, ~)
        @routine begin
            ly ← one(ULogarithmic{T})
            lx ← one(ULogarithmic{T})
            lx *= convert(x)
            for i=1:n
                ly *= x
            end
        end
        out += convert(ly)
        ~@routine
    end
end

```


Since the fixed-point number is not reversible under \ast , naive checkpointing would require stack operations inside a loop. With reversible thinking, we can convert the fixed-point number to logarithmic numbers to utilize the reversibility of \ast as shown in Listing. 14. Here, the algorithm to convert a regular fixed-point number to a logarithmic number can be efficient. (Turner, 2010)

C IMPLEMENTATION OF AD IN NiLANG

To backpropagate the program, we first reverse the code through source code transformation and then insert the gradient code through operator overloading. If we inline all the functions in Listing. 4, the function body would be like Listing. 15. The automatically generated inverse program (i.e. $(y, x) \rightarrow (y - \log(x), x)$) would be like Listing. 16.

Listing 15: The inlined function body of Listing. 4.

```
@routine begin
  nsq ← zero(T)
  n ← zero(T)
  nsq += x[i].re ^ 2
  nsq += x[i].im ^ 2
  n += sqrt(nsq)
end
y![i].re += log(n)
y![i].im += atan(x[i].im, x[i].re)
~@routine
```

Listing 16: The inverse of Listing. 15.

```
@routine begin
  nsq ← zero(T)
  n ← zero(T)
  nsq += x[i].re ^ 2
  nsq += x[i].im ^ 2
  n += sqrt(nsq)
end
y![i].re -= log(n)
y![i].im -= atan(x[i].im, x[i].re)
~@routine
```

To compute the adjoint of the computational process in Listing. 15, one simply insert the gradient code into its inverse in Listing. 16. The resulting inlined code is show in Listing. 17.

Listing 17: Insert the gradient code into Listing. 16, the original computational processes are highlighted in yellow background.

```
@routine begin
  nsq ← zero(GVar{T,T})
  n ← zero(GVar{T,T})

  gsqa ← zero(T)
  gsqa += x[i].re.x ^ 2
  x[i].re.g -= gsqa * nsq.g
  gsqa -= nsq.x ^ 2
  gsqa -= x[i].re.x ^ 2
  gsqa → zero(T)
  nsq.x += x[i].re.x ^ 2

  gsqb ← zero(T)
  gsqb += x[i].im.x ^ 2
  x[i].im.g -= gsqb * nsq.g
  gsqb -= x[i].im.x ^ 2
  gsqb → zero(T)
  nsq.x += x[i].im.x ^ 2

  @zeros T ra rb
  rta += sqrt(nsq.x)
  rb += 2 * ra
  nsq.g -= n.g / rb
  rb -= 2 * ra
```

```
ra -= sqrt(nsq.x)
~@zeros T ra rb
n.x += sqrt(nsq.x)
end
y![i].re.x -= log(n.x)
n.g += y![i].re.g / n.x

y![i].im.x -= atan(x[i].im.x, x[i].re.x)
@zeros T xy2 jac_x jac_y
xy2 += abs2(x[i].re.x)
xy2 += abs2(x[i].im.x)
jac_y += x[i].re.x / xy2
jac_x += (-x[i].im.x) / xy2
x[i].im.g += y![i].im.g * jac_y
x[i].re.g += y![i].im.g * jac_x
jac_x -= (-x[i].im.x) / xy2
jac_y -= x[i].re.x / xy2
xy2 -= abs2(x[i].im.x)
xy2 -= abs2(x[i].re.x)
~@zeros T xy2 jac_x jac_y
~@routine
```

Here, `@zeros TYPE var1 var2...` is the macro to allocate multiple variables of the same type. Its inverse operations starts with `~@zeros` deallocates zero emptied variables. In practice, “inserting gradients” is not achieved by source code transformation, but by operator overloading. We change the element type to a composite type `GVar` with two fields, value `x` and gradient `g`. With multiple dispatching primitive instructions on this new type, values and gradients can be updated simultaneously. Although the code looks much longer, the computing time (with reversibility check closed) is not.

Listing 18: Time and allocation to differentiate complex valued log.

```

julia> @inline function (ir_log)(x::Complex{T}) where T
    log(abs(x)) + im*angle(x)
end

julia> @btime ir_log(x) setup=(x=1.0+1.2im); # native code
30.097 ns (0 allocations: 0 bytes)

julia> @btime (@instr y += log(x)) setup=(x=1.0+1.2im; y=0.0+0.0im); # reversible code
17.542 ns (0 allocations: 0 bytes)

julia> @btime (@instr ~(y += log(x))) setup=(x=GVar(1.0+1.2im, 0.0+0.0im); y=GVar(0.1+0.2im, 1.0+0.0im)); # adjoint code
25.932 ns (0 allocations: 0 bytes)

```

The performance is unreasonably good because the generated Julia code is further compiled to LLVM so that it can enjoy existing optimization passes. For example, the optimization passes can find out that for an irreversible device, uncomputing local variables `n` and `nsq` to zeros does not affect return values, so that it will ignore the uncomputing process automatically. Unlike checkpointing based approaches that focus a lot in the optimization of data caching on a global stack, NiLang does not have any optimization pass in itself. Instead, it throws itself to existing optimization passes in Julia. Without accessing the global stack, NiLang’s code is quite friendly to optimization passes. In this case, we also see the boundary between source code transformation and operator overloading can be vague in a Julia, in that the generated code can be very different from how it looks.

The joint functions for primitive instructions `(:+=)(sqrt)` and `(:-=)(sqrt)` used above can be defined as in Listing. 19.

Listing 19: Adjoints for primitives `(:+=)(sqrt)` and `(:-=)(sqrt)`.

```

@i @inline function (:-=)(sqrt)(out::GVar, x::GVar{T}) where T
    @routine @invcheckoff begin
        @zeros T a b
        a += sqrt(x.x)
        b += 2 * a
    end
    out!.x -= a
    x.g += out!.g / b
    ~@routine
end

```

D MORE BENCHMARKS

D.1 SPARSE MATRICES

We benchmarked the call, uncall and backward propagation time used for sparse matrix dot product and matrix multiplication. Here, we estimate the time for back propagating gradients rather than including both forward and backward, since `mul!` does not output a scalar as loss.

	dot	mul! (complex valued)
Julia-O	3.493e-04	8.005e-05
NiLang-O	4.675e-04	9.332e-05
NiLang-B	5.821e-04	2.214e-04

Table 2: Absolute runtimes in seconds for computing the objectives (O) and the backward pass (B) of sparse matrix operations. The matrix size is 1000×1000 , and the element density is 0.05. The total time used in computing gradient can be estimated by summing “O” and “B”.

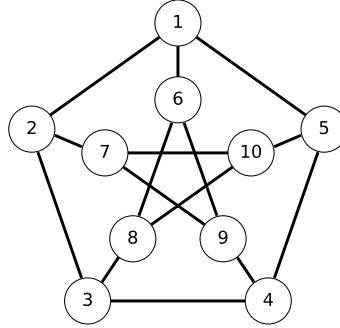


Figure 5: The Petersen graph has 10 vertices and 15 edges. We want to find a minimum embedding dimension for it.

The time used for computing backward pass is approximately 1.5-3 times the Julia’s native forward pass. This is because the instruction length of differentiating basic arithmetic instructions is longer than pure computing.

D.2 GRAPH EMBEDDING PROBLEM

Graph embedding can be used to find a proper representation for an order parameter (Takahashi & Sandvik, 2020) in condensed matter physics. People want to find a minimum Euclidean space dimension k that a Petersen graph can embed into, that the distances between pairs of connected vertices are l_1 , and the distance between pairs of disconnected vertices are l_2 , where $l_2 > l_1$. The Petersen graph is shown in Fig. 5. Let us denote the set of connected and disconnected vertex pairs as L_1 and L_2 , respectively. This problem can be variationally solved with the following loss.

$$\begin{aligned} \mathcal{L} = & \text{Var}(\text{dist}(L_1)) + \text{Var}(\text{dist}(L_2)) \\ & + \exp(\text{relu}(\overline{\text{dist}(L_1)} - \overline{\text{dist}(L_2)} + 0.1))) - 1 \end{aligned} \quad (7)$$

The first line is a summation of distance variances in two sets of vertex pairs, where $\text{Var}(X)$ is the variance of samples in X . The second line is used to guarantee $l_2 > l_1$, where \bar{X} means taking the average of samples in X . Its reversible implementation could be found in our benchmark repository.

We repeat the training for dimension k from 1 to 10. In each training, we fix two of the vertices and optimize the positions of the rest. Otherwise, the program will find the trivial solution with overlapped vertices. For $k < 5$, the loss is always much higher than 0, while for $k \geq 5$, we can get a loss close to machine precision with high probability. From the $k = 5$ solution, it is easy to see $l_2/l_1 = \sqrt{2}$. An Adam optimizer with a learning rate 0.01 (Kingma & Ba) requires ~ 2000 steps training. The trust region Newton’s method converges much faster, which requires ~ 20 computations of Hessians to reach convergence. Although training time is comparable, the converged precision of the later is much better.

Since one can combine ForwardDiff and NiLang to obtain Hessians, it is interesting to see how much performance we can get in differentiating the graph embedding program.

In Table 3, we show the the performance of different implementations by varying the dimension k . The number of parameters is $10k$. As the baseline, (a) shows the time for computing the function call. We have reversible and irreversible implementations, where the reversible program is slower than the irreversible native Julia program by a factor of ~ 2 due to the uncomputing overhead. The reversible program shows the advantage of obtaining gradients when the dimension $k \geq 3$. The larger the number of inputs, the more advantage it shows due to the overhead proportional to input size in forward mode AD. The same reason applies to computing Hessians, where the combo of NiLang and ForwardDiff gives the best performance for $k \geq 3$.

k	2	4	6	8	10
Julia-O	4.477e-06	4.729e-06	4.959e-06	5.196e-06	5.567e-06
NiLang-O	7.173e-06	7.783e-06	8.558e-06	9.212e-06	1.002e-05
NiLang-U	7.453e-06	7.839e-06	8.464e-06	9.298e-06	1.054e-05
NiLang-G	1.509e-05	1.690e-05	1.872e-05	2.076e-05	2.266e-05
ReverseDiff-G	2.823e-05	4.582e-05	6.045e-05	7.651e-05	9.666e-05
ForwardDiff-G	1.518e-05	4.053e-05	6.732e-05	1.184e-04	1.701e-04
Zygote-G	5.315e-04	5.570e-04	5.811e-04	6.096e-04	6.396e-04
(NiLang+F)-H	4.528e-04	1.025e-03	1.740e-03	2.577e-03	3.558e-03
ForwardDiff-H	2.378e-04	2.380e-03	6.903e-03	1.967e-02	3.978e-02
(ReverseDiff+F)-H	1.966e-03	6.058e-03	1.225e-02	2.035e-02	3.140e-02

Table 3: Absolute times in seconds for computing the objectives (O), uncall objective (U), gradients (G) and Hessians (H) of the graph embedding program. k is the embedding dimension, the number of parameters is $10k$.

E PORTING NiLANG TO ZYGOTE

Zygote is a popular machine learning package in Julia. We can port NiLang’s automatically generated backward rules to Zygote to accelerate some performance-critical functions. The following example shows how to speed up the backward propagation of `norm` by ~ 50 times.

Listing 20: Porting NiLang to Zygote.

```

julia> using Zygote, NiLang, NiLang.AD, BenchmarkTools, LinearAlgebra

julia> x = randn(1000);

julia> @benchmark norm'(x)
BenchmarkTools.Trial:
  memory estimate:  339.02 KiB
  allocs estimate:  8083
  -----
  minimum time:     228.967 μs (0.00% GC)
  median time:      237.579 μs (0.00% GC)
  mean time:        277.602 μs (12.06% GC)
  maximum time:     5.552 ms (94.00% GC)
  -----
  samples:          10000
  evals/sample:     1

julia> @i function r_norm(out::T, out2::T, x::AbstractArray{T}) where T
    for i=1:length(x)
        @inbounds out2 += x[i]^2
    end
    out += sqrt(out2)
end

julia> Zygote.@adjoint function norm(x::AbstractArray{T}) where T
    # compute the forward with regular norm (might be faster)
    out = norm(x)
    # compute the backward with NiLang's norm, element type is GVar
    out, dy -> (grad((~r_norm)(GVar(out, dy), GVar(out^2), GVar(x))[3]),)
end

julia> @benchmark norm'(x)
BenchmarkTools.Trial:
  memory estimate:  23.69 KiB
  allocs estimate:  2
  -----
  minimum time:     4.015 μs (0.00% GC)
  median time:      5.171 μs (0.00% GC)
  mean time:        6.872 μs (13.00% GC)
  maximum time:     380.953 μs (93.90% GC)
  -----
  samples:          10000
  evals/sample:     7

```

We first import the `norm` function from Julia standard library `LinearAlgebra`. Zygote’s builtin AD engine will generate a slow code and memory allocation of 339KB. Then we write a reversible norm function `r_norm` with NiLang and port the backward function to Zygote by specifying the backward rule (the function marked with macro `Zygote.@adjoint`). Except for the speed up in computing time, the memory allocation also decreases to 23KB, which is equal to the sum of the original x and the array used in backpropagation.

$$(1000 \times 8 + 1000 \times 8 \times 2) / 1024 \approx 23$$

The later one has a doubled size because `GVar` has an extra gradient field.

F ERROR ANALYSIS

Running reversible programming with the floating pointing number system can introduce round-off errors and make the program not reversible. The quantify the effects, we use the leapfrog integrator to compute the orbitals of planets in our solar system as a benchmark. The leapfrog iterations can be represented as

$$\vec{d}_i = G \frac{m_j(\vec{x}_j - \vec{x}_i)}{\|\vec{x}_i - \vec{x}_j\|^3} \quad (8)$$

$$\vec{v}_{i+1/2} = \vec{v}_{i-1/2} + \vec{d}_i \Delta t \quad (9)$$

$$\vec{x}_{i+1} = \vec{x}_i + \vec{v}_{i+1/2} \Delta t \quad (10)$$

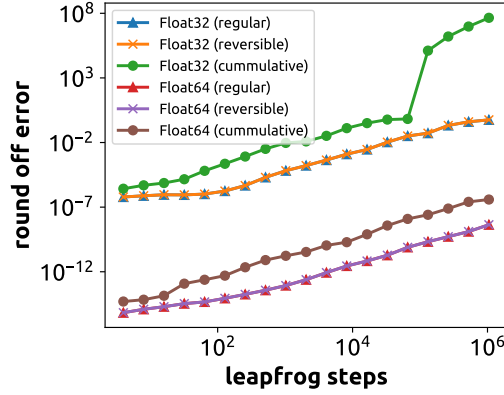


Figure 6: Round-off errors in the final axes of planets as a function of the number of time steps. “(regular)” means an irreversible program, “(reversible)” means a reversible program (Listing. 21), and “(accumulative)” means a reversible program with the acceleration computed with accumulative errors (Listing. 22).

where G is the gravitational constant and m_j is the mass of j th planet, \vec{x} , \vec{v} and \vec{a} are location, velocity and acceleration respectively. The first value of velocity is $v_{1/2} = a_0 \Delta t / 2$. Since the dynamics of our solar system are symplectic and the leapfrog integrator is time-reversible, the reversible program does not have overheads and the evolution time can go arbitrarily long with constant memory. We compare the mean error in the final axes of the planets and show the results in Fig. 6. Errors are computed by comparing with the results computed with high precision floating-point numbers. One of the key steps that introduce round-off error is the computation of acceleration. If it is implemented as in Listing. 21, the round-off error does not bring additional effect in the reversible context, hence we see overlapping lines “(regular)” and “(reversible)” in the figure. This is because, when returning a dirty (not exactly zero cleared due to the floating-point round-off error) ancilla to the ancilla pool, the small remaining value will be zero-cleared automatically in NiLang. The acceleration function can also be implemented as in Listing. 22, where the same variable `rb` is repeatedly used for compute and uncompute, the error will accumulate on this variable. In both Float64 (double precision floating point) and Float32 (single precision floating point) benchmarks, the results show a much lower precision. Hence, simulating reversible programming with floating-point numbers does not necessarily make the results less reliable if one can avoid cumulative errors in the implementation.

Listing 21: Compute the acceleration. Compute and uncompute on ancilla `rc`

```
@i function :(+)= (acceleration)(y!::V3{T},
  ra::V3{T}, rb::V3{T}, mb::Real, G)
  where T
  @routine @invcheckoff begin
    @zeros T d anc1 anc2 anc3 anc4
    rc ← zero(V3{T})
    d += sqdistance(ra, rb)
    anc1 += sqrt(d)
    anc2 += anc1 ^ 3
    anc3 += G * mb
    anc4 += anc3 / anc2
    rc += rb - ra
  end
  y! += anc4 * rc
  ~@routine
end
```

Listing 22: Compute the acceleration. Compute and uncompute on the input variable `rb`.

```
@i function :(+)= (acceleration)(y!::V3{T},
  ra::V3{T}, rb::V3{T}, mb::Real, G)
  where T
  @routine @invcheckoff begin
    @zeros T d anc1 anc2 anc3 anc4
    d += sqdistance(ra, rb)
    anc1 += sqrt(d)
    anc2 += anc1 ^ 3
    anc3 += G * mb
    anc4 += anc3 / anc2
    rb -= ra
  end
  y! += anc4 * rb
  ~@routine
  # rb is not recovered rigorously!
end
```